INTERNATIONAL JOURNAL OF ADVANCED RESEARCH
International Peer-Reviewed Research Journal
ISSN (Online): 3106-7980 | ISSN (Print): 3106-7972
Volume 3 • Issue 4 • August 2026

SCATTERING BY PEMC CYLINDER COATED WITH POROUS SAND

M. Imran Shahzad[*1], M. Saddique[2], Sania Shaheen[3], Mudassar Hussain[4] , Saeed Ahmed[5]

[*1,2,3]*Department of Physics, Federal Urdu University of Arts, Sciences and Technology, Islamabad, Pakistan,*
[4]*Department of Physics, NFC Institute of Engineering and Technology, Multan,Pakistan,*
[5]*Department of Electronics, Quaid-i-Azam University, Islamabad, Pakistan,*

[*1]ishahzad@fuuast.edu.pk, [2]msaddique@fuuast.edu.pk, [3]sania.shaheen@fuuast.edu.pk,
[4]mudassar.hussain@nfciet.edu.pk, [5]saeedqau@gmail.com

DOI: https://doi.org/10.5281/zenodo.24100223

Keywords
Scattering by PEMC, circular cylinder coated with porous sand, parallel and perpendicular polarization.

Article History
Received: *01 July 2026*
Accepted: *15 August 2026*
Published: *31 August 2026*

Copyright @Author
Corresponding Author:
***M. Imran Shahzad**

Abstract
The electromagnetic scattering of an incident uniform plane wave from a circular PEMC cylinder covered with porous sand is investigated theoretically. The research takes into account polarization situations that are both parallel and perpendicular. A comparison is made with the sand-coated cylinder's back scattering cross-section. The monostatic and bistatic echo widths for the co-polarized and cross-polarized fields have been computed for a number of PEMC cylinders covered with porous sands. For the specific cases of PMC (perfect magnetic conductor) ($M\eta c=0$) and PEC (perfect electric conductor) ($M\eta c=\infty$), echo widths have been computed and compared to the PEMC coated cylinder. Compared to similarly coated PEC and PMC cylinders, the coated PEMC has a smaller radar cross-section (RCS). A comparison between the numerical results and the available literature reveals a high degree of agreement.

INTRODUCTION

Researchers have found electromagnetic wave scattering from circular cylinders to be an intriguing subject [1, 2]. Lindell's introduction of perfect electromagnetic conductor (PEMC) material [3] has drawn the interest of numerous researchers [4–16]. PEMC materials are a generalization of perfect magnetic conductor (PMC) and perfect electromagnetic conductor (PEC) materials. The PEMC boundary conditions are,

$$\vec{n} \times \left(\vec{H} + M\vec{E}\right) = 0 \quad (1)$$

$$\vec{n}.\left(\vec{D} - M\vec{B}\right) = 0 \quad (2)$$

where M represents the PEMC boundary's admittance, and $\vec{D} = \epsilon\vec{E}$ and $\vec{B} = \mu\vec{H}$ are the host medium's permittivity and permeability, respectively. A lot of research has been done on the issue of electromagnetic waves scattering from concentrically coated materials [17–20]. If a scattering obstacle is composed of layers or portions of multiple materials, the scattering behavior becomes significantly more complex. We will examine and contrast our research with that of Li and Shen [22] about how a conductive cylinder covered in porous sand scatters electromagnetic plane waves. This research examines electromagnetic scattering from a circular cylinder coated in porous sand that is infinite in both PEC and PMC. The electric vector of the incident plane wave is taken both parallel to and perpendicular to To simplify the challenge, a homogenous layer of different materials of

uniform thickness is applied to the axis of the infinite long PEC and PMC circular cylinder. The theoretical investigation makes use of the eigenfunction expansion method. The problem is formulated under the assumption that fields exist in two regions: the coating with a distinct material layer and the open space outside. At the two interfaces, suitable boundary conditions are implemented. The large argument approximation of the Hankel function is used to compute the far scattered field patterns. The numerical findings are compared with the published work for the special situations to confirm the accuracy of the analytical formulation and the numerical code. The temporal dependence $e^{-j\omega t}$, which we have employed in this study, has been suppressed throughout the analysis.

Mathematical Model

The geometry of the scattering problem is shown in $Fig\ 1$. It contains a PEMC circular cylinder which has been coated by porous sand $(\theta = 0.3, 0.4, 0.5)$ where θ is the porousity of the sand along with its permittivity and permeability.

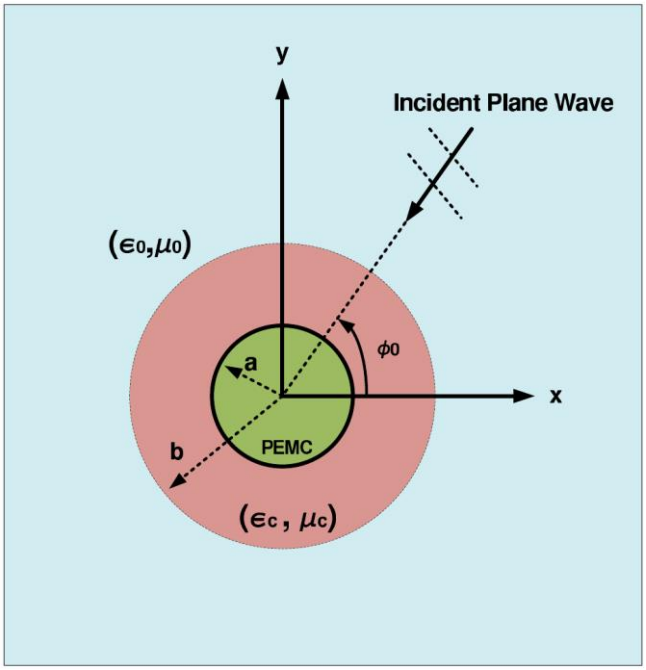


Figure 1: Plane wave scattered by PEMC Cylinder Coated with Porous Sand

The coating on PEC and PMC cylinders is thought to be uniformly thick. It is intended for the coated cylinder to have an indefinite extent. The cylinder's radius is a, while the coated cylinder's radius is b. In Fig. 1, $region\ 0$ refers to the external medium $\rho > b$, which is open space (μ_0, ϵ_0) . $region\ 0's$ wave number is $k_0 = \omega\sqrt{\mu_0\epsilon_0}$. With wave number $k_c = \omega\sqrt{\mu_c\epsilon_c}$, the material region, $a < \rho < b$ and (μ_1, ϵ_1) , is referred to as $region\ 1$. The perpendicular and parallel polarizations of the incident plane wave are covered individually in the next two subsections. Here we use coating materials as porous sands with specified values as:

$(\epsilon = 17.48, \theta = 0.3, \sigma = 8.106 \times 10^{-}4),$
$(\epsilon = 25.601, \theta = 0.4, \sigma = 1.44 \times 10^{-}3)$ and
$(\epsilon = 35.265, \theta = 0.5, \sigma = 2.252 \times 10^{-}3).$

where θ represents the porousity of the sand and σ the conductivity of the sand, similarly ϵ indicates the electric constant of the sand.

INTERNATIONAL JOURNAL OF ADVANCED RESEARCH
International Peer-Reviewed Research Journal
ISSN (Online): 3106-7980 | ISSN (Print): 3106-7972
Volume 3 • Issue 4 • August 2026

Parallel Polarization

In terms of the cylindrical coordinates (ρ, ϕ), the incident electric field when its polarization is parallel to the cylinders' axis, can be written as follows:

$$E_{0z}^{inc}(\rho,\phi) = E_0 e^{jk_0\rho cos\phi} \quad (3)$$

An infinite Fourier-Bessel series can be used to express the incident field using the wave transformation as follows:

$$E_{0z}^{inc} = E_0 \sum_{n=-\infty}^{\infty} j^n J_n(k_0\rho) e^{jn\phi} \quad (4)$$

The appropriate ϕ component of the magnetic field can be found using the Maxwell equation as follows:

$$H_{0\phi}^{inc} = -E_0/j\eta_0 \sum_{n=-\infty}^{\infty} j^n J_{n'}(k_0\rho) e^{jn\phi} \quad (5)$$

where $\eta_0 = \sqrt{\mu_0/\epsilon_0}$ is the impedance of free space, $J_n(.)$ represents the first kind Bessel function with prime as the derivative with respect to the entire argument. Since a PEC and PMC cylinder is the main component, accordingly, the scattered fields in $region\ 0$ can be expressed as follows using Maxwell's equation:

$$E_{0z}^{s} = E_0 \sum_{n=-\infty}^{\infty} j^n a_n^{TM} H_n^{(2)}(k_0\rho) e^{jn\phi} \quad (6)$$

$$H_{0\phi}^{s} = -\frac{1}{j\eta_0} E_0 \sum_{n=-\infty}^{\infty} j^n a_n^{TM} H_n^{(2)'}(k_0\rho) e^{jn\phi} \quad (7)$$

$$H_{0z}^{s} = -\frac{j}{\eta_0} E_0 \sum_{n=-\infty}^{\infty} j^n b_n^{TM} H_n^{(2)}(k_0\rho) e^{jn\phi} \quad (8)$$

$$E_{0\phi}^{s} = -E_0 \sum_{n=-\infty}^{\infty} j^n b_n^{TM} H_n^{(2)'}(k_0\rho) e^{jn\phi} \quad (9)$$

The fields in $region\ 1$, which is a uniform-thickness material coating surrounded by two interfaces at values $\rho = a$ and $\rho = b$, can be written as follows:

$$E_{1z} = E_0 \sum_{n=-\infty}^{\infty} j^n [c_n^{TM} J_n(k_c\rho) + d_n^{TM} Y_n(k_c\rho)] e^{jn\phi} \quad (10)$$

$$H_{1\phi} = -\frac{1}{j\eta_c} E_0 \sum_{n=-\infty}^{\infty} j^n [c_n^{TM} J_n'(k_c\rho) + d_n^{TM} Y_n'(k_c\rho)] e^{jn\phi} \quad (11)$$

$$H_{1z} = -\frac{j}{\eta_c} E_0 \sum_{n=-\infty}^{\infty} j^n [e_n^{TM} J_n(k_c\rho) + f_n^{TM} Y_n(k_c\rho)] e^{jn\phi} \quad (12)$$

$$E_{1\phi} = -E_0 \sum_{n=-\infty}^{\infty} j^n [e_n^{TM} J_n'(k_c\rho) + f_n^{TM} Y_n'(k_c\rho)] e^{jn\phi} \quad (13)$$

$J_n(x)$ and $N_n(x)$ are the first and second-kind Bessel functions in each of the aforementioned equations, and $H_n^{(1)}(x) = J_n(x) + iN_n(x)$ and $H_n^{(2)}(x) = J_n(x) - iN_n(x)$. The six unknown scattering coefficients a_n^E, b_n^E, c_n^E, d_n^E, e_n^E, and f_n^E for the TM incident plane wave that need to be ascertained are also included in the aforementioned expressions. By applying suitable boundary conditions at the interfaces $\rho = a$ and $\rho = b$ these unknowns can be determined. At the interface $\rho = a$, the boundary conditions are:

$$H_{1z} + ME_{1z} = 0, \quad \rho = a, 0 \le \phi \le 2\pi \quad (14)$$

$$H_{1\phi} + ME_{1\phi} = 0, \quad \rho = a, 0 \le \phi \le 2\pi \quad (15)$$

And the boundary conditions at the interface $\rho = b$, are:

$$E_{0z}^{inc} + E_{0z}^{s} = E_{1z}, \quad \rho = b, 0 \le \phi \le 2\pi \quad (16)$$

$$H_{0\phi}^{inc} + H_{0\phi}^{s} = H_{1\phi}, \quad \rho = b, 0 \le \phi \le 2\pi \quad (17)$$

$$H_{0z}^{s} = H_{1z}, \quad \rho = b, 0 \le \phi \le 2\pi \quad (18)$$

$$E_{0\phi}^{s} = E_{1\phi}, \quad \rho = b, 0 \le \phi \le 2\pi \quad (19)$$

A linear matrix equation for the unknown scattering coefficients is obtained by applying these boundary conditions at $\rho = a$ and $\rho = b$. All the unknown scattering coefficients values can be obtained by solving the following matrix equation.

$$\begin{pmatrix} a_n^{TM} \\ b_n^{TM} \\ c_n^{TM} \\ d_n^{TM} \\ e_n^{TM} \\ f_n^{TM} \end{pmatrix} = \begin{pmatrix} 0 & 0 & \beta j J_n(k_c a) & \beta j Y_n(k_c a) & J_n(k_c a) & Y_n(k_c a) \\ 0 & 0 & J_n'(k_c a) & Y_n'(k_c a) & \beta j J_n'(k_c a) & \beta j Y_n'(k_c a) \\ -H_n^{(2)}(k_0 b) & 0 & J_n(k_c b) & Y_n(k_c b) & 0 & 0 \\ -\zeta H_n^{(2)\prime}(k_0 b) & 0 & J_n'(k_c b) & Y_n'(k_c b) & 0 & 0 \\ 0 & -\zeta H_n^{(2)}(k_0 b) & 0 & 0 & J_n(k_c b) & Y_n(k_c b) \\ 0 & -H_n^{(2)\prime}(k_0 b) & 0 & 0 & J_n'(k_c b) & Y_n'(k_c b) \end{pmatrix}^{-1} \begin{pmatrix} 0 \\ 0 \\ J_n(k_0 b) \\ \zeta J_n'(k_0 b) \\ 0 \\ 0 \end{pmatrix} \tag{20}$$

Using the values of a_n^E and b_n^E The scattered fields emitted by the coated PEC and PMC cylinders are obtained in equations (6) and (9), respectively. Using the asymptotic version of Hankel functions leads to far-zone scattered fields. The ratio of the total power scattered by the scatterer to the incident power per unit area on the scatterer is known as the backscattering cross-section, and it is expressed as follows:

$$\sigma = 2\pi\rho W^{sca} W^{inc} = 2\pi\rho |E^s|^2 |E^{inc}|^2 \tag{21}$$

where W^{inc}, the incident power density and W^{sca}, is the far-zone power density. Using the large argument approximation of the Hankel function, the normalized bistatic echo width in the case of TM plane wave incidence can be expressed as follows:

$$\sigma_{co}/\lambda_0 = 2\pi \left| \sum_{n=-\infty}^{\infty} a_n^{TM} e^{jn\phi} \right|^2 \tag{22}$$

$$\sigma_{cross}/\lambda_0 = 2\pi \left| \sum_{n=-\infty}^{\infty} b_n^{TM} e^{jn\phi} \right|^2 \tag{23}$$

where a_n^{TM} and b_n^{TM}, are the coefficients of the scattering of co- polarized and cross-polarized field components respectively.

Perpendicuar Polarization

The incident magnetic field can be represented as follows when the incident field is polarized perpendicular to the cylinders' axes:

$$H_{0z}^{inc}(\rho, \phi) = H_0 e^{jk_0 \rho \cos\phi} \tag{24}$$

where H_0, is the magnetic field's incident amplitude. The incident magnetic field's wave transformation into an infinite Fourier-Bessel series leads to,

$$H_{0z}^{inc}(\rho, \phi) = H_0 \sum_{n=-\infty}^{\infty} j^n J_n(k_0 \rho) e^{jn\phi} \tag{25}$$

the ϕ component of the magnetic field, Using Maxwell equation, , is given as:

$$E_{0\phi}^{inc}(\rho, \phi) = -j\eta_0 H_0 \sum_{n=-\infty}^{\infty} j^n J_{n\prime}(k_0 \rho) e^{jn\phi} \tag{26}$$

The scattered field, in response to this incident magnetic field, in $region\ 0$, may be expressed as:

$$H_{0z}^s = H_0 \sum_{n=-\infty}^{\infty} j^n a_n^{TE} H_n^{(2)}(k_0 \rho) e^{jn\phi} \tag{27}$$

$$E_{0\phi}^s = -j\eta_0 H_0 \sum_{n=-\infty}^{\infty} j^n a_n^{TE} H_n^{(2)\prime}(k_0 \rho) e^{jn\phi} \tag{28}$$

$$E_{0z}^s = j\eta_0 H_0 \sum_{n=-\infty}^{\infty} j^n b_n^{TE} H_n^{(2)}(k_0 \rho) e^{jn\phi} \tag{29}$$

$$H_{0\phi}^s = -H_0 \sum_{n=-\infty}^{\infty} j^n b_n^{TE} H_n^{(2)\prime}(k_0 \rho) e^{jn\phi} \tag{30}$$

In the bounded region 1, the fields are given as:

$$H_{1z} = H_0 \sum_{n=-\infty}^{\infty} j^n [c_n^{TE} J_n(k_c \rho) + d_n^{TE} Y_n(k_c \rho)] e^{jn\phi} \tag{31}$$

$$E_{1\phi} = -j\eta_1 H_0 \sum_{n=-\infty}^{\infty} j^n [c_n^{TE} J_n'(k_c \rho) + d_n^{TE} Y_n'(k_c \rho)] e^{jn\phi} \tag{32}$$

$$E_{1z} = j\eta_1 H_0 \sum_{n=-\infty}^{\infty} j^n [e_n^{TE} J_n(k_c \rho) + f_n^{TE} Y_n(k_c \rho)] e^{jn\phi} \tag{33}$$

$$H_{1\phi} = -H_0 \sum_{n=-\infty}^{\infty} j^n [e_n^{TE} J_n'(k_c\rho) + f_n^{TE} Y_n'(k_c\rho)] e^{jn\phi} \quad (34)$$

where $a_n^{TE}, b_n^{TE}, c_n^{TE}, d_n^{TE}, e_n^{TE}$, and f_n^{TE} are the six unknown scattering coefficients when the incident plane wave is polarized perpendicularly. These are determined using the boundary conditions at the two interfaces i.e. at $\rho = a$ and at $\rho = b$. The boundary conditions at the interface $\rho = a$ are:

$$H_{1z} + ME_{1z} = 0, \quad \rho = a, 0 \le \phi \le 2\pi \quad (35)$$

$$H_{1\phi} + ME_{1\phi} = 0, \quad \rho = a, 0 \le \phi \le 2\pi \quad (36)$$

And the boundary conditions at $\rho = b$, are:

$$H_{0z}^{inc} + H_{0z}^{s} = H_{1z}, \quad \rho = b, 0 \le \phi \le 2\pi \quad (37)$$

$$E_{0\phi}^{inc} + E_{0\phi}^{s} = E_{1\phi}, \quad \rho = b, 0 \le \phi \le 2\pi \quad (38)$$

$$E_{0z}^{s} = E_{1z}, \quad \rho = b, 0 \le \phi \le 2\pi \quad (39)$$

$$H_{0\phi}^{s} = H_{1\phi}, \quad \rho = b, 0 \le \phi \le 2\pi \quad (40)$$

Applying Boundary conditions Using the values of the incident and scattered field components, we obtain a matrix of linear equations in the set of boundary conditions mentioned above. Solution of this matrix gives the unknown scattering coefficients.

International Journal of Advanced Research

$$\begin{pmatrix} a_n^{TE} \\ b_n^{TE} \\ c_n^{TE} \\ d_n^{TE} \\ e_n^{TE} \\ f_n^{TE} \end{pmatrix} = \begin{pmatrix} 0 & 0 & J_n(k_c a) & Y_n(k_c a) & \beta j J_n(k_c a) & \beta j Y_n(k_c a) \\ 0 & 0 & \beta j J_n'(k_c a) & \beta j Y_n'(k_c a) & J_n'(k_c a) & Y_n'(k_c a) \\ -H_n^{(2)}(k_0 b) & 0 & J_n(k_c b) & Y_n(k_c b) & 0 & 0 \\ -H_n^{(2)\prime}(k_0 b) & 0 & \zeta J_n'(k_c b) & \zeta Y_n'(k_c b) & 0 & 0 \\ 0 & -H_n^{(2)}(k_0 b) & 0 & 0 & \zeta J_n(k_c b) & \zeta Y_n(k_c b) \\ 0 & -H_n^{(2)\prime}(k_0 b) & 0 & 0 & J_n'(k_c b) & Y_n'(k_c b) \end{pmatrix}^{-1} \begin{pmatrix} 0 \\ 0 \\ J_n(k_0 b) \\ J_n'(k_0 b) \\ 0 \\ 0 \end{pmatrix} \quad (41)$$

When TE plane wave incidence occurs, the normalized bistatic echo width can be expressed as follows:

$$\sigma_{co}/\lambda_0 = 2\pi \left| \sum_{n=-\infty}^{\infty} a_n^H e^{jn\phi} \right|^2 \quad 42)$$

$$\sigma_{cross}/\lambda_0 = 4\pi \left| \sum_{n=-\infty}^{\infty} b_n^H e^{jn\phi} \right|^2 \quad (43)$$

where a_n^H and b_n^H, are the coefficients of the scattering of co- polarized and cross-polarized field components rspectively, when the suggested configuration is excited by an incident field that is perpendicularly polarized.

INTERNATIONAL JOURNAL OF ADVANCED RESEARCH
International Peer-Reviewed Research Journal
ISSN (Online): 3106-7980 | ISSN (Print): 3106-7972
Volume 3 • Issue 4 • August 2026

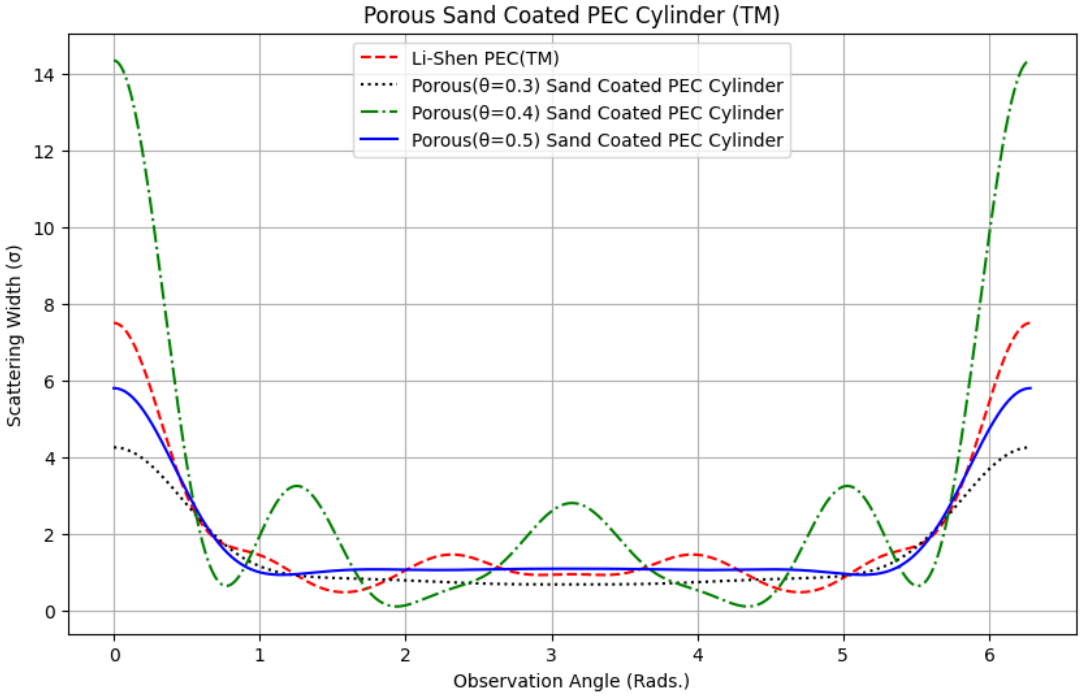


Figure 2: For the admittance M=∞ in TM polarizations, Porous Sand $(\boldsymbol{\theta = 0.3, 0.4, 0.5})$ coated PEMC core $\boldsymbol{\mu_c = 1}$, $\boldsymbol{f = 1GHz}$, and $\boldsymbol{\lambda = 0.3}$.

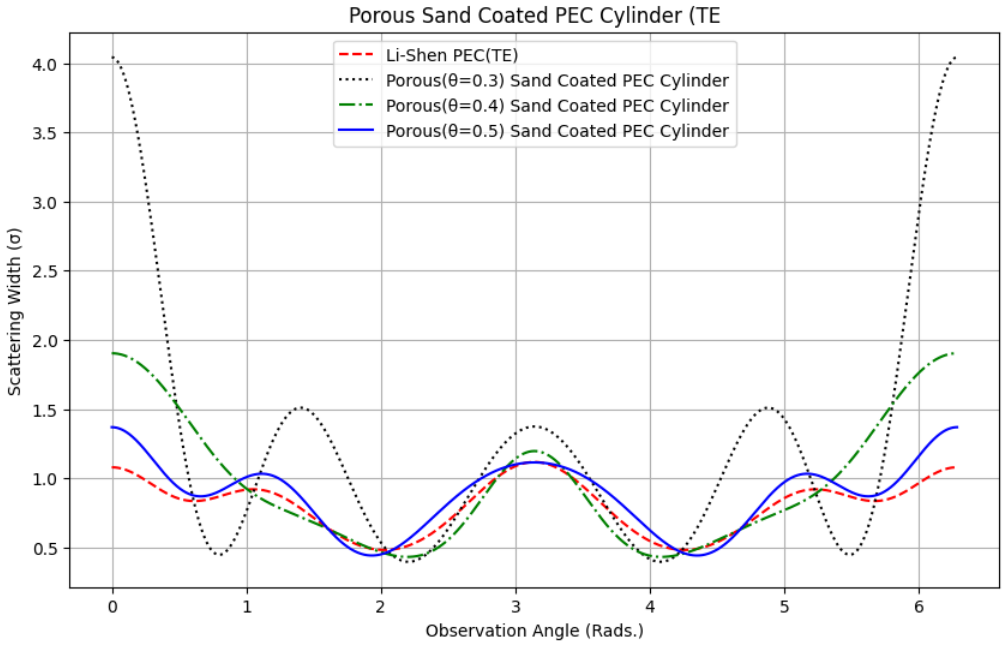


Figure 3: For the admittance M=∞ in TM polarizations, Porous Sand $(\boldsymbol{\theta = 0.3, 0.4, 0.5})$ coated PEMC core $\boldsymbol{\mu_c = 1}$, $\boldsymbol{f = 1GHz}$, and $\boldsymbol{\lambda = 0.3}$.

INTERNATIONAL JOURNAL OF ADVANCED RESEARCH
International Peer-Reviewed Research Journal
ISSN (Online): 3106-7980 | ISSN (Print): 3106-7972
Volume 3 • Issue 4 • August 2026

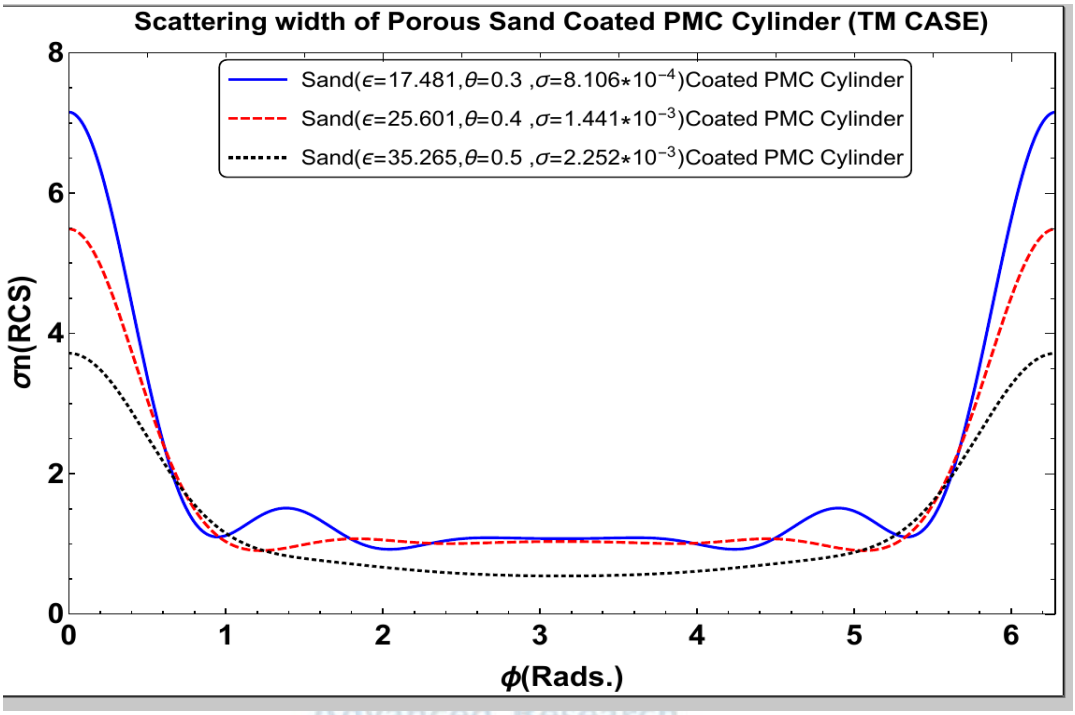


Figure 4: For the admittance M=∞ in TM polarizations, Porous Sand($\boldsymbol{\theta = 0.3, 0.4, 0.5}$) coated PEMC core $\boldsymbol{\mu_c = 1}$, $\boldsymbol{f = 1GHz}$, and $\boldsymbol{\lambda = 0.3}$.

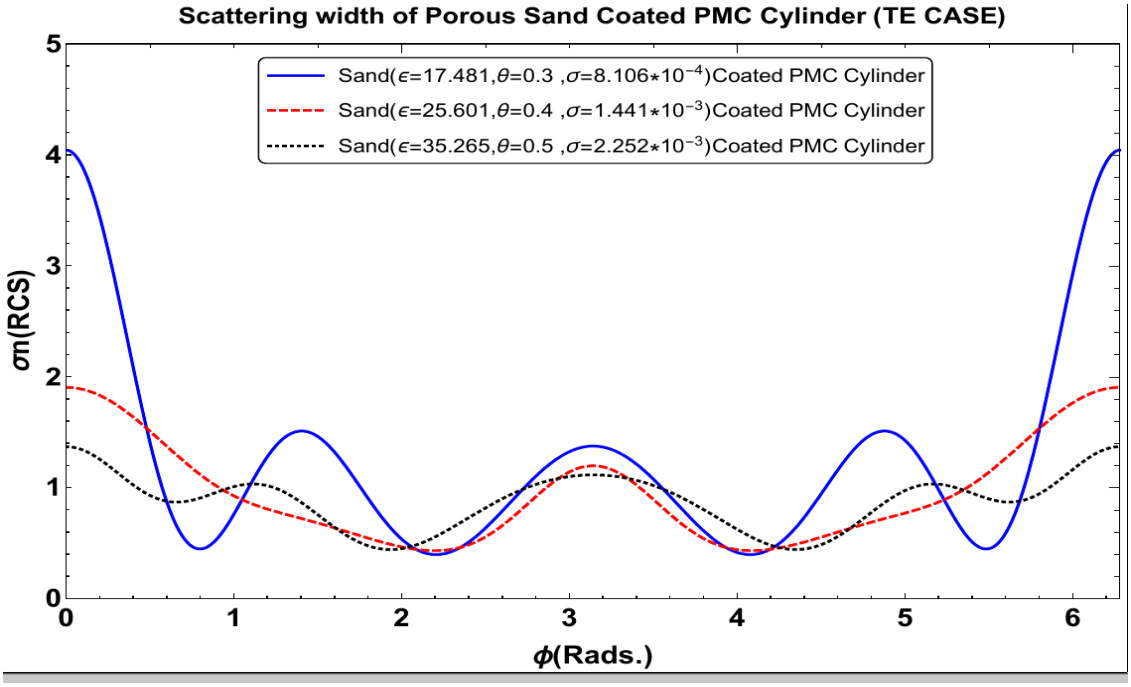


Figure 5: For the admittance M=∞ in TM polarizations, Porous Sand ($\boldsymbol{\theta = 0.3, 0.4, 0.5}$) coated PEMC core $\boldsymbol{\mu_c = 1}$, $\boldsymbol{f = 1GHz}$, and $\boldsymbol{\lambda = 0.3}$.

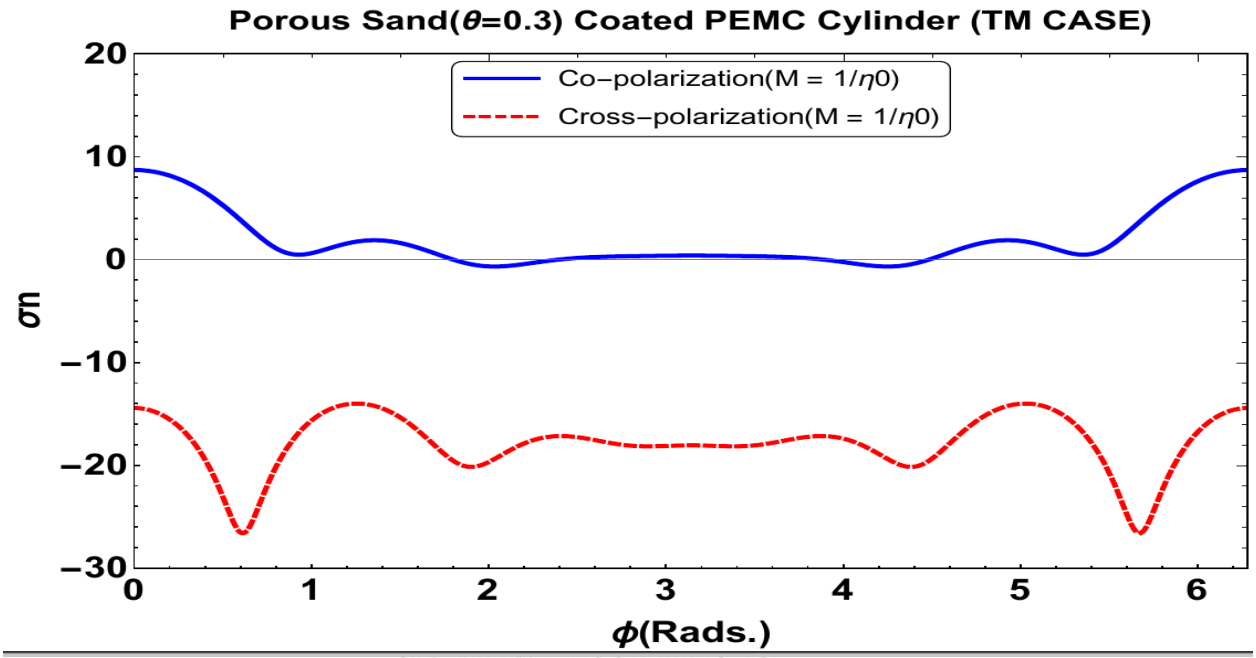


Figure 6: Effect of PEMC parameter on scattering width for Porous Sands $(\boldsymbol{\theta = 0.3})$-coated cylinder for both Co-polarized and cross-polarization as a function of normalized PEMC parameter $\boldsymbol{M\eta_1 = 1}$ at $\boldsymbol{f = 1}$ GHz.

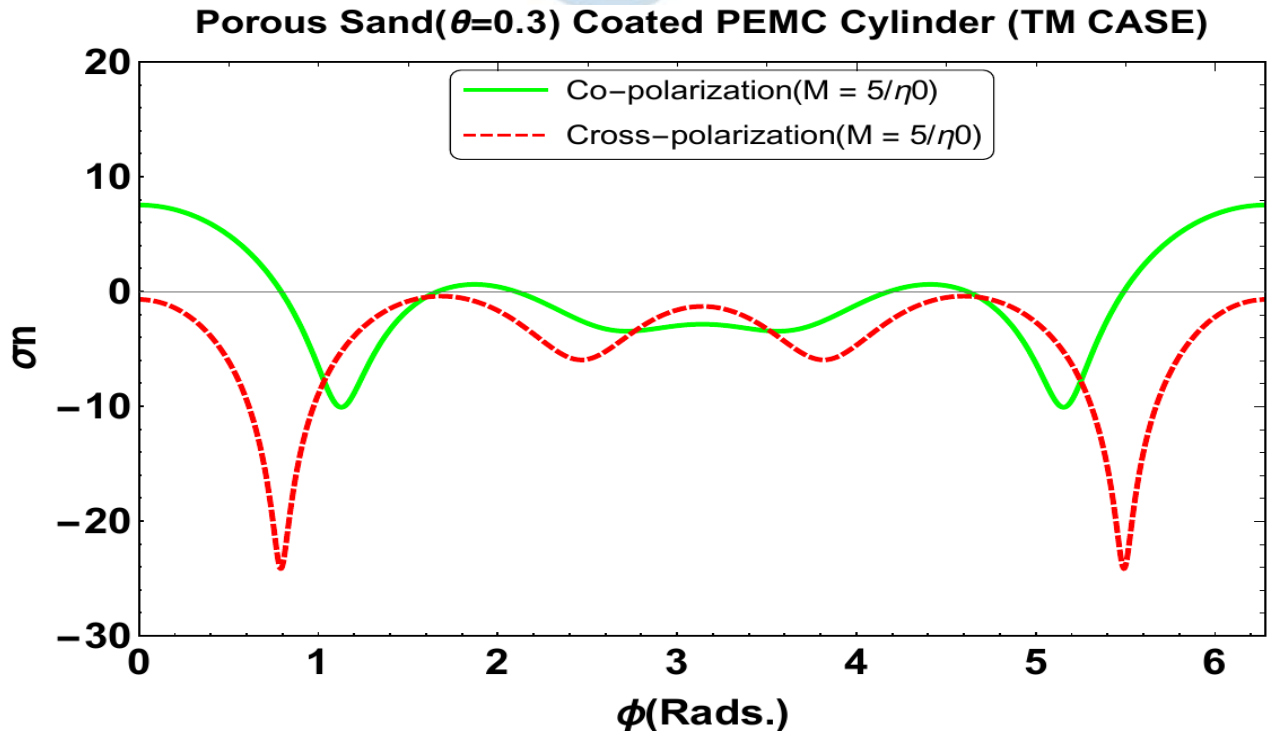


Figure 7: Effect of PEMC parameter on scattering width for Porous Sands $\boldsymbol{\theta = 0.3}$-coated cylinder for both Co-polarized and cross-polarization as a function of normalized PEMC parameter $\boldsymbol{M\eta_1 = 5}$ at $\boldsymbol{f = 1}$ GHz.

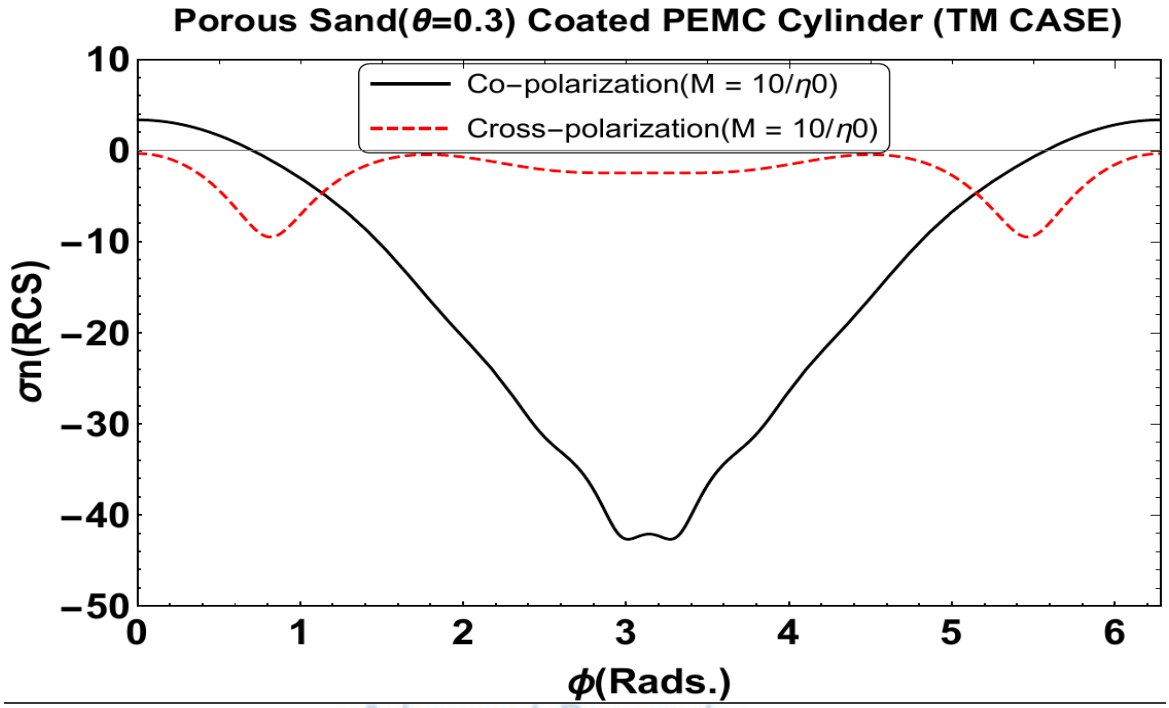


Figure 8: Effect of PEMC parameter on scattering width for Porous Sands $(\boldsymbol{\theta = 0.3})$-coated cylinder for both Co-polarized and cross-polarization as a function of normalized PEMC parameter $\boldsymbol{M\eta_1 = 10}$ at $\boldsymbol{f = 1}$ GHz.

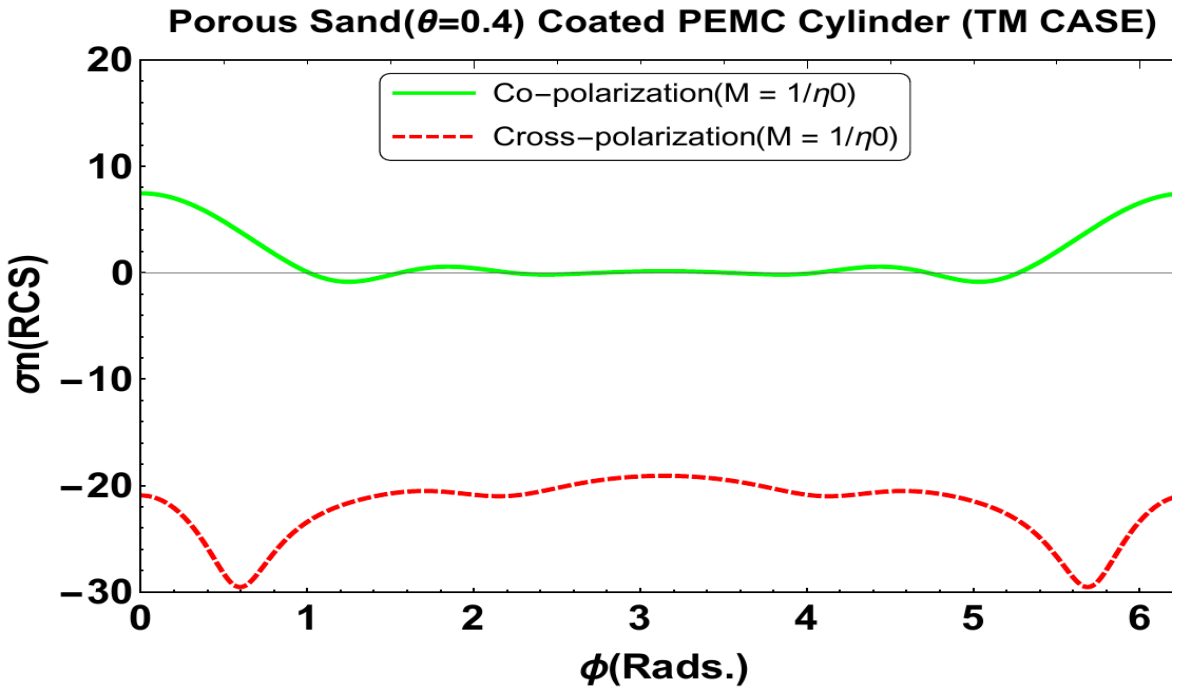


Figure 9: Effect of PEMC parameter on scattering width for Porous Sands $(\boldsymbol{\theta = 0.4})$-coated cylinder for both Co-polarized and cross-polarization as a function of normalized PEMC parameter $\boldsymbol{M\eta_1 = 5}$ at $\boldsymbol{f = 1}$ GHz.

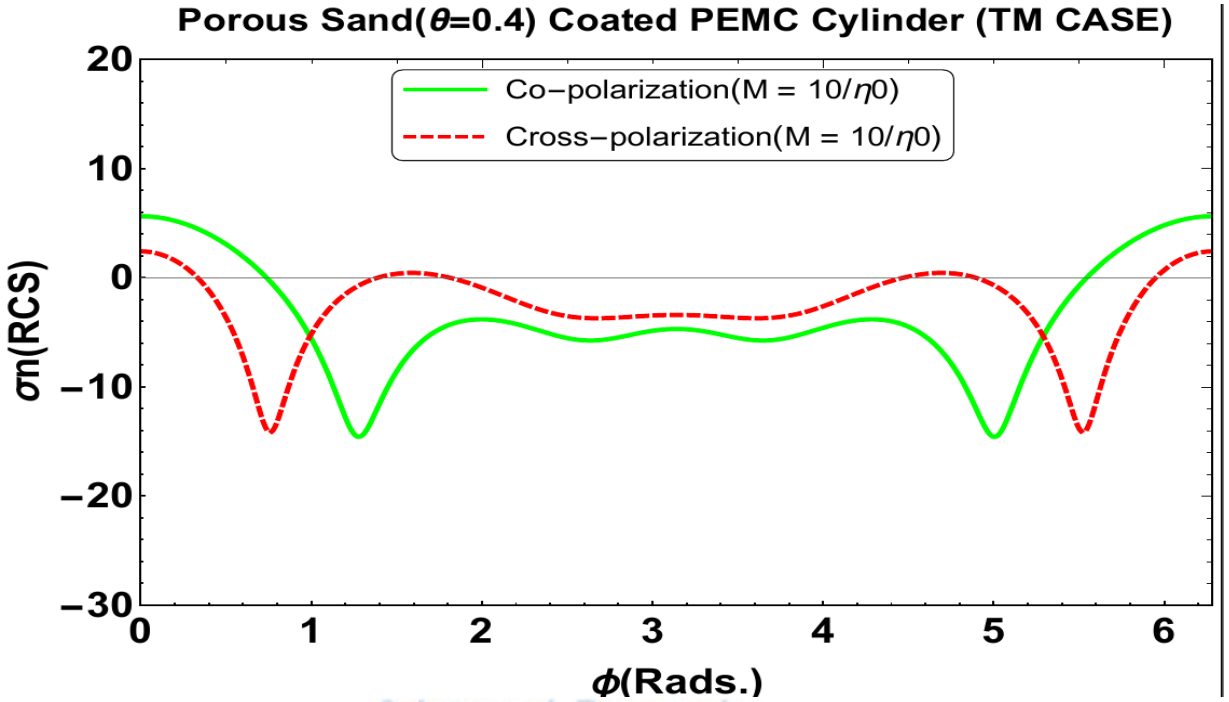


Figure 10: Effect of PEMC parameter on scattering width for Porous Sands $(\boldsymbol{\theta = 0.4})$-coated cylinder for both Co-polarized and cross-polarization as a function of normalized PEMC parameter $\boldsymbol{M\eta_1 = 5}$ at $\boldsymbol{f = 1}$ GHz.

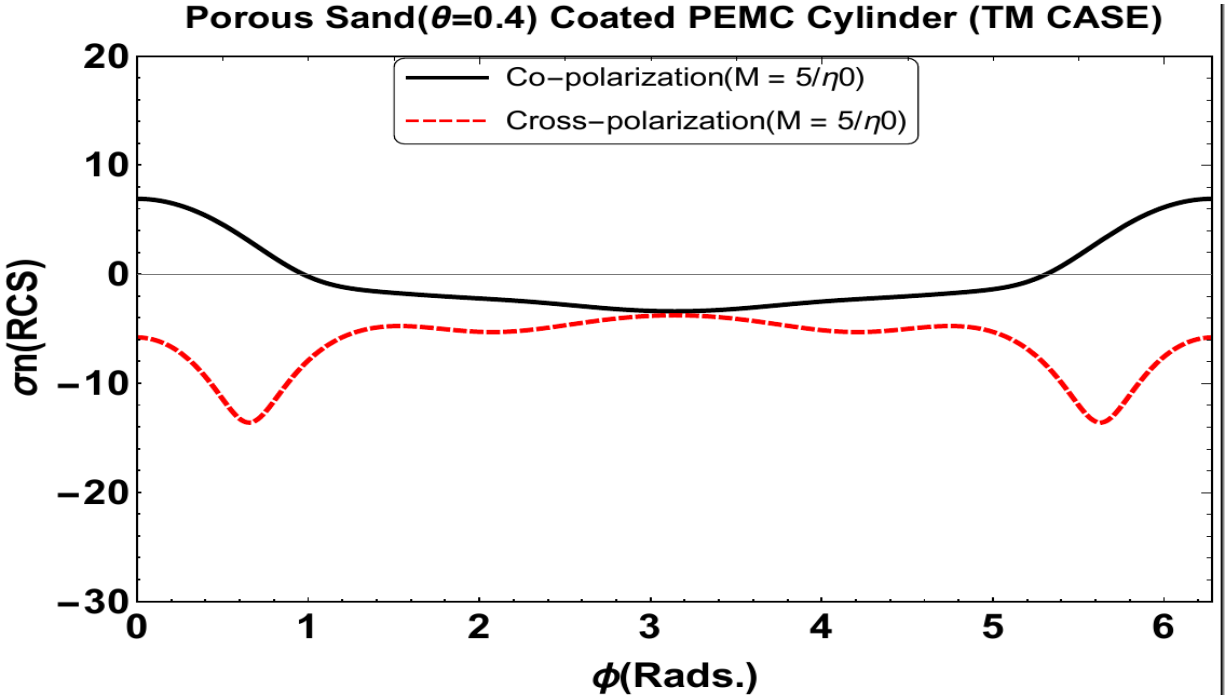


Figure 11: Effect of PEMC parameter on scattering width for Porous Sands $(\boldsymbol{\theta = 0.4})$-coated cylinder for both Co-polarized and cross-polarization as a function of normalized PEMC parameter $\boldsymbol{M\eta_1 = 5}$ at $\boldsymbol{f = 1}$ GHz.

INTERNATIONAL JOURNAL OF ADVANCED RESEARCH
International Peer-Reviewed Research Journal
ISSN (Online): 3106-7980 | ISSN (Print): 3106-7972
Volume 3 • Issue 4 • August 2026

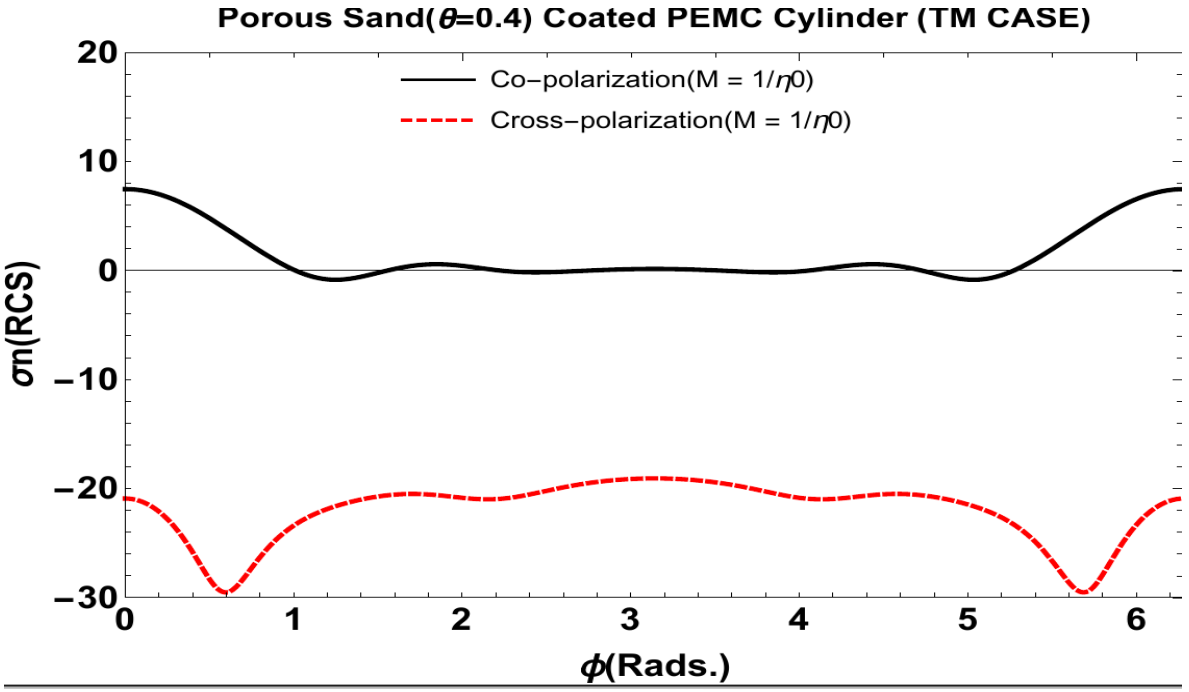


Figure 12: Effect of PEMC parameter on scattering width for Porous Sands $(\boldsymbol{\theta = 0.5})$-coated cylinder for both Co-polarized and cross-polarization as a function of normalized PEMC parameter $\boldsymbol{M\eta_1 = 10}$ at $\boldsymbol{f = 1}$ GHz.

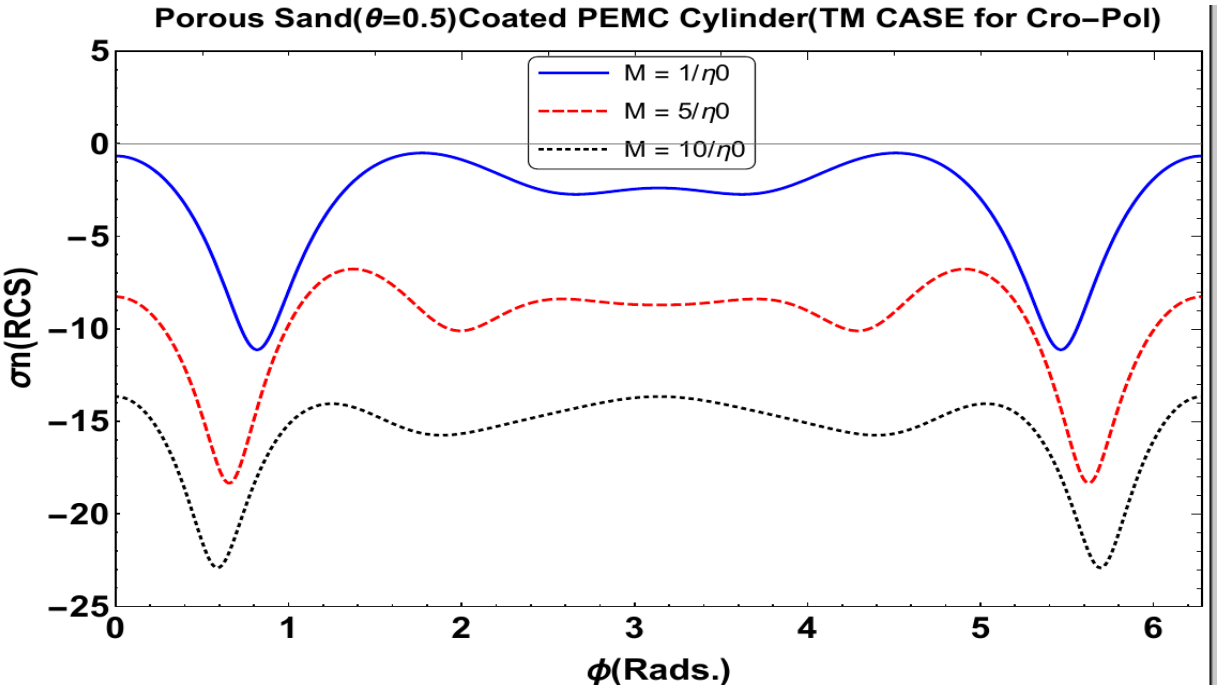


Figure 13: Effect of PEMC parameter on scattering width for Porous Sands $(\boldsymbol{\theta = 0.5})$-coated cylinder for both Co-polarized and cross-polarization as a function of normalized PEMC parameter $\boldsymbol{M\eta_1 = 1, 5, 10}$ at $\boldsymbol{f = 1}$ GHz.

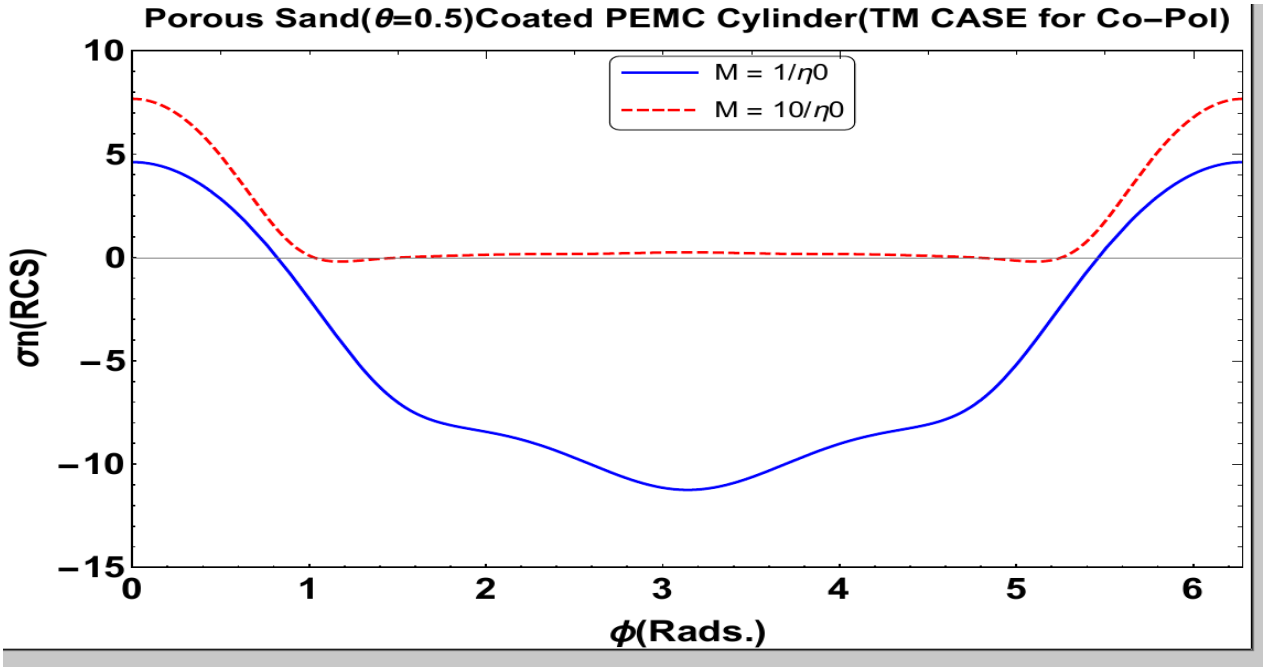


Figure 14: Effect of PEMC parameter on scattering width for Porous Sands $(\boldsymbol{\theta = 0.5})$-coated cylinder for both Co-polarized and cross-polarization as a function of normalized PEMC parameter $\boldsymbol{M\eta_1 = 1, 10}$ at $\boldsymbol{f = 1}$ GHz.

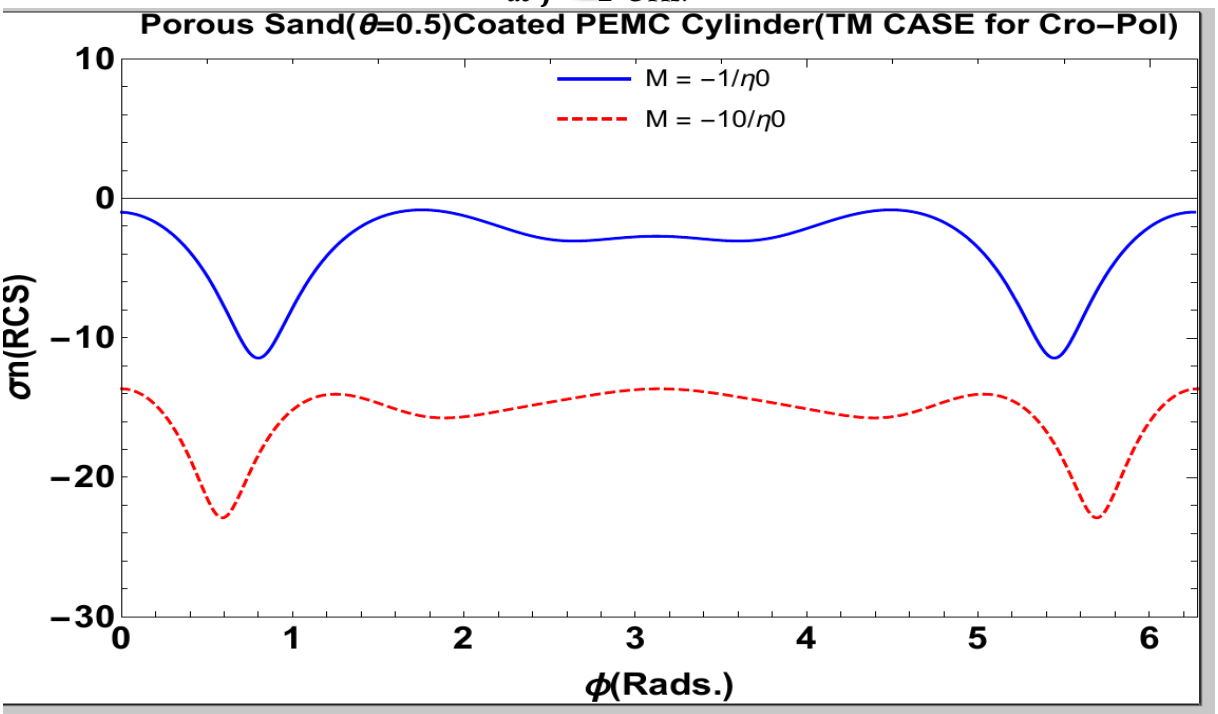


Figure 15: Effect of PEMC parameter on scattering width for Porous Sands $(\boldsymbol{\theta = 0.5})$-coated cylinder for both Co-polarized and cross-polarization as a function of normalized PEMC parameter $\boldsymbol{M\eta_1 = -1, -10}$ at $\boldsymbol{f = 1}$ GHz.

Numerical Results and Discussion

In this section we have presented the scattering back scattering cross section and numerical results of a material-coated circular cylinder made of PEC and PMC. The acquired results are compared with those reported in published literature to validate the analytical formulation and the numerical code. It is discovered that the comparison is in perfect accord. The PEC and PMC cylinder and coating radii are taken to be a=5 cm and b=10 cm, respectively, in all plots, while the frequency of the incident field is taken as $f = 1\mathrm{G}Hz$.

In $Fig.2$ The normalized bistatic echo widths of the Porous Sand coated PEMC core that behaves like a PMC core for the admittance M=0 in TM polarizations are compared in Fig. 3 with the normalized bistatic echo widths of the Porous Sand coated PEMC core that behaves like a PEC core. In $Fig.2$, Porous Sands $(\theta = 0.3,0.4,0.5)$ coated PEMC core $\mu_c = 1$, $f = 1GHz$, and $\lambda = 0.3$. In $Fig.3$ The normalized bistatic echo widths of the Porous Sand coated PEMC core that behaves like a PMC core for the admittance M=0 in TE polarizations are compared in Fig. 3 with the normalized bistatic echo widths of the Porous Sand coated PEMC core that behaves like a PEC core. In $Fig.3$ Porous Sands $(\theta = 0.3,0.4,0.5)$ coated PEMC core $\mu_c = 1$, $f = 1GHz$, and $\lambda = 0.3$. In $Fig.3$, the normalized bistatic echo widths of the Porous Sand coated PEMC core that behaves likes PEC core for the The Comparison between the normalized bistatic echo widths of the POrous Sand coated PEMC core that behaves likes PMC core for the admittance $M = 0$ in TM polarizations. In this figure Porous Sands $(\theta = 0.3, 0.4, 0.5)$ coated PEMC core $\mu_c = 1$, $f = 1GHz$, and $\lambda = 0.3$. In $Fig.4$, we have a compared the normalized bistatic echo widths of the Porous Sand coated PEMC core that behaves likes PMC core for the admittance $M = 0$ in TM polarizations. In this figure Porous Sands $(\theta = 0.3, 0.4, 0.5)$ coated PEMC core $\mu_c = 1$, $f = 1GHz$, and $\lambda = 0.3$. In $Fig.5$, we have a compared the normalized bistatic echo widths of the Porous Sand coated PEMC core that behaves likes PMC core for the admittance $M = 0$ in TE polarizations. In this figure Porous Sands $(\theta = 0.3, 0.4, 0.5)$ coated PEMC core $\mu_c = 1$, $f = 1GHz$, and $\lambda = 0.3$. In $Fig.6-12$, we have analized the effect of PEMC parameters on scattering width for Porous Sands $(\theta = 0.3)$-coated cylinder for both Co-polarized and cross-polarization as a function of normalized PEMC parameter $M\eta_1 = 1,5,10$ at $f = 1$ GHz. In $Fig.13$, we have analized the effect of PEMC parameters on scattering width for Porous Sands $(\theta = 0.3)$-coated cylinder for both Co-polarized and cross-polarization as a function of normalized PEMC parameter $M\eta_1 = 1,5,10$ at $f = 1$ GHz. In $Fig.14$, we have analized the effect of PEMC parameters on scattering width for Porous Sands $(\theta = 0.3)$-coated cylinder for both Co-polarized and cross-polarization as a function of normalized PEMC parameter $M\eta_1 = 1,10$ at $f = 1$ GHz.

In $Fig.15$, we have analized the effect of PEMC parameters on scattering width for Porous Sands $(\theta = 0.3)$ coated cylinder for both Co-polarized and cross-polarization as a function of normalized PEMC parameter $M\eta_1 = -1,-10,\ f = 1$ GHz.

Conclusion

This study developed analytical formulations and conducted numerical simulations to analyze electromagnetic wave scattering by a perfect electromagnetic conductor PEC and PMC cylinder coated with Porous Sands $(\theta = 0.3, 0.4, 0.5)$. To validate the accuracy of the analytical approach and numerical implementation, the results were compared with previously published works under specific scenarios. The monostatic and bistatic echo widths for the co-polarized and the cross-polarized fields were computed for various porous sands coated PEMC cylinder. Echo widths for the special cases of perfect electric conductor $(M\eta_c = \infty)$, and perfect magnetic conductor $(M\eta_c = 0)$ cores were computed and were compared to the PEMC coated cylinder. It is found that the the coated PEMC has a reduced radar cross-section (RCS) in comparison with the similarly coated PEC and PMC cylinders. The computed results of the presented formulations are found in good agreement with the published results of some special cases confirm the validity and accuracy of the presented analysis.

REFERENCES

[1] Cincoti, G., Gori, F., Santarsiero, M., Frezza, F., Furno, F., and Schettini, G., "Plane wave expansion of cylindrical functions," Opt. Commun., Vol. 95, pp. 192-198, Jan. 1993.

[2] Muhammad A. Mushref, "Closed solution to electromagnetic scattering of a plane wave by an eccentric cylinder coated with metamaterials," Optics Communications 270 (2007) 441-446.

[3] Lindell, I. V., and Sihvola, A. H., "Perfect electromagnetic conductor," J. Electromagn. Waves Appl., Vol. 19, No. 7, 861-869, 2005.

[4] Hehl, F. W. and Obukhov, Y. N., "Linear media in classical electrodynamics and post constraint," Phys. Lett. A, Vol. 334, 249-259, 2005.

[5] Obukhov, Y. N. and Hehl, F. W., "Measuring a piecewise constant axion field in classical electrody-namics," Phys. Lett. A, Vol. 341, 357-365, 2005.

[6] Lindell, I. V., and Sihvola, A. H., "Realization of the PEMC boundary," IEEE Trans. Antennas Propag., Vol. 53, No. 9, 3012-3018, 2005.

[7] Lindell, I. V., and Sihvola, A. H., "Transformation method for problems involving perfect electromagnetic conductor (PEMC) structures," IEEE Trans. on Antennas and Propagation, Vol. 53, No. 9, 3005-3011, 2005.

[8] Ruppin, R., "Scattering of electromagnetic radiation by a perfect electromagnetic conductor cylinder," Journal of Electromagnetic Waves and Applications, Vol. 20, No. 13, 1853-1860, 2006.

[9] Lindell, I. V., and Sihvola, A. H., "Losses in PEMC boundary," IEEE Trans. on Antennas and Propagation, Vol. 54, No. 9, 2553-2558, 2006.

[10] Lindell, I. V., and Sihvola, A. H., "The PEMC resonator," J. Electromagn. Waves Appl., Vol. 20, No. 7, 849-859, 2006.

[11] Jancewicz, B., "Plane electromagnetic wave in PEMC," Electromagn. Waves Appl., Vol. 20, No. 5, 647-659, 2006.

[12] Hussain, A., and Naqvi, Q. A., "Perfect electromagnetic conductor (pemc) and fractional waveguide," Progress In Electromagnetics Research, PIER 73, 61-69, 2007.

[13] Hussain, A., Naqvi, Q. A. and Abbas, M., "Fractional duality and perfect electromagnetic conductor," Progress In Electromagnetics Research, Vol. 71, 85-94, 2007.

[14] Ahmed, S., and Naqvi, Q. A., "Electromagnetic scattering from a perfect electromagnetic conductor cylinder buried in a dielectric half space," Progress In Electromagnetics Research, PIER 78, 25-38, 2008.

[15] Ahmed, S., and Naqvi, Q. A., "Electromagnetic scattering form parallel perfect electromagnetic conductor cylinders of circular cross-sections using iterative procedure,"J. of Electromagn. Waves and Appl., Vol. 22, 987-1003, 2008.

[16] Fiaz, M. A., Ghaffar, A., and Naqvi, Q.A., "High frequency expressions for the field in the caustic region of a PEMC cylindrical reflector using Maslov's method," J. Electromagn. Waves Appl., Vol. 20, No. 5, 647-659, 2006.

[17] Massoudi, H., Damaskos, N. J., and Uslenghi, P. L. E., Scattering by a composite and anisotropic circular cylindrical structures, Electromagnetics, Vol. 8, 71-83, 1988.

[18] Kishk, A. A., Parrikar, R. P., and Elsherbeni, A. Z., Electromagnetic scattering from an eccentric multilayered circular cylinder, IEEE Trans. on Antennas and Propagation, Vol. AP-40, 295-303, 1992.

[19] Shen, Z. X., Electromagnetic scattering by an impedance cylinder coated eccentrically with a chiroplasma cylinder,IEE Pro. Microwaves, Antennas and Propagation, Vol. 141, 279-284, Aug. 1994.

International Journal of Advanced Research

[20] Shen, Z. and Li, C.,"Electromagnetic scattering by a conducting cylinder coated with metamaterials," Progress In Electromagnetics Research, PIER 42, 91-105, 2003.

International Journal of Advanced Research